Journal

Highlights

Full Title of the Paper

First Author, Second Author

- First key contribution.
- Second key contribution.
- Third key contribution.

Full Title of the Paper

First Author[a], Second Author[a,*]

[a] *Institution Name, Department, Address, City, Country.*

ARTICLE INFO

Keywords:
Keyword1
Keyword2
Keyword3

ABSTRACT

...

1. Introduction

Ensuring the safety, serviceability, and life extension of existing civil structures has fostered a rapid diffusion of Structural Health Monitoring (SHM) systems, with an increasing number of infrastructures being continuously instrumented. Among SHM strategies, vibration-based monitoring is particularly attractive due to its non-destructive nature and relatively low deployment cost. Within this context, SHM strategies can be broadly classified into data-driven and model-based approaches. Data-based approaches utilize modal parameters extracted from measurements (frequencies, mode shapes, damping) and infer their variations as indicators of structural condition. Model-based approaches, instead, use such modal data to update structural models in such a way that deviations of the updated parameters can be mapped to location and severity of damage. However, the latter family of methods critically depends on the availability of a high-fidelity numerical model, which is not always feasible in practice since design or assessment models often incorporate simplifications such as idealized boundary conditions, rigid joints, or lumped masses that limit their predictive capability.

To address this issue, this work proposes a transfer learning methodology between structures of similar typology. The idea is to exploit monitoring data and the high-fidelity (HF) finite element model (FEM) available for one reference structure to enrich low-fidelity (LF) models of other, similar structures. The methodology is demonstrated on two laboratory-scale steel portal frames with comparable geometry and structural configuration, located at the Universities of Granada (UGR) and Perugia (UNIPG). For the UGR frame (see Fig. 1), both LF and HF models are developed and calibrated against experimentally identified modal data. On this basis, a surrogate model is developed from both LF–HF models, learning the mapping between LF and HF responses. The resulting surrogate model is then used to upgrade the LF model of the Perugia frame. The results show that the transferred surrogate significantly improves the quality of the Perugia LF model in terms of modal prediction, thereby enabling the application of model-based damage identification even in the absence of a fully detailed FEM. These findings pave the way for population-based SHM strategies, where knowledge accumulated on a subset of well-characterized assets can be systematically reused to enhance the monitoring of structurally similar infrastructures.

The modal characteristics of each of the structures (real, HF and LF) of the UGR frame are summarized in Table 1.

2. Lumped Model

2.0.1. Stiffness matrix

Description: Centre of mass (CM) is assumed to coincide with the center of rigidity (CR); each floor acts as a rigid diaphragm; four identical columns of constant section at the corners of a $B \times H$ rectangle;the base is clamped.

Three dofs are retained per floor at the center of mass (CM): in-plane translations U_X, U_Y and rotation R_Z: $\mathbf{q} = [U_{X,1\ldots5},\ U_{Y,1\ldots5},\ R_{Z,1\ldots5}]^T$, see Fig 2a.

Direction X (shear-building idealization): Each story is represented by a lateral spring equal to the sum of the 4 fixed–fixed columns acting in X. Consequently, the bloc of the stiffness matrix along these dofs reads:

*Corresponding author
author@email.com (F. Author); second@email.com (S. Author)
ORCID(s): 0000-0000-0000-0000 (F. Author); 0000-0000-0000-0000 (S. Author)

ID	Mode type	OMA (acc) [Hz]	HF [Hz]	LF [Hz]	Error HF [%]	Error LF [%]
1	1st x-bending	2.610	2.546	1.732	-2.47	-33.66
2	1st y-bending	3.798	3.962	3.235	4.32	-14.82
3	torsional	7.641	7.927	3.417	3.74	-55.28
4	2nd x-bending	8.099	7.786	5.008	-3.87	-38.17
5	3rd x-bending	12.901	12.607	7.856	-2.28	-39.11
6	4th x-bending	16.438	16.427	9.867	-0.07	-39.97
7	5th x-bending	18.720	19.629	11.036	4.85	-41.05
8	2nd y-bending	20.876	19.863	19.598	-4.85	-6.12

Table 1
Modal data for real structure, HF and LF models.

$$K_{xx} = \begin{bmatrix} 2k_x & -k_x & 0 & 0 & 0 \\ -k_x & 2k_x & -k_x & 0 & 0 \\ 0 & -k_x & 2k_x & -k_x & 0 \\ 0 & 0 & -k_x & 2k_x & -k_x \\ 0 & 0 & 0 & -k_x & k_x \end{bmatrix}, \qquad k_x = 4\,\frac{12\,E\,I_x}{L_c^3}. \tag{1}$$

Direction Y (cantilever beam) Each column is modeled as an Euler–Bernoulli (EB) cantilever beam with five traslational degrees of freedom (one per floor). The stiffness matrix of each cantilever beam $K_{yy}^{(\mathrm{col,eff})}$ is obtained from the assembling of five BE elements and (static) condensation of the rotational degrees of freedom. Under a rigid diaphragm, floor translations are identical across the four columns, hence the lateral stiffness in Y is $K_{yy} = 4\,K_{yy}^{(\mathrm{col,eff})}$:

$$K_{yy}^{(\mathrm{col,eff})} = \frac{EI}{181\,L_c^3} \begin{bmatrix} 3408 & -2154 & 864 & -216 & 36 \\ -2154 & 2652 & -1938 & 756 & -126 \\ 864 & -1938 & 2544 & -1722 & 468 \\ -216 & 756 & -1722 & 1788 & -660 \\ 36 & -126 & 468 & -660 & 291 \end{bmatrix}, \qquad K_{yy} = 4\,K_{yy}^{(\mathrm{col,eff})}. \tag{2}$$

Torsion about Z (per-floor torsional stiffness). For corner supports at $(\pm B/2, \pm H/2)$ and uniform lateral stiffness in each direction, the torsional floor stiffness equals the sum of lateral springs weighted by the squared lever arms:

$$K_{tt} = \tfrac{H^2}{4}\,K_{xx} + \tfrac{B^2}{4}\,K_{yy} \tag{3}$$

Global stiffness (block form). Under the symmetry/CM=CR assumption the global stiffness matrix reads:

$$\mathbf{K} = \mathrm{diag}\big(K_{xx},\ K_{yy},\ K_{tt}\big) \tag{4}$$

2.0.2. Generated acceleration time series

- Random forces on the 15 dofs of the structure.
- State space equations solved for the derived K and M matrices.
- Sampling frequency at 207s (same as accelerometers' data).
- Recorded along 15 directions shown in Figure 3 (i.e. from the original DOFs, the values on the "virtual" accelerometers have been obtained by imposing Rigid Body Motion conditions).
- Noise added with SNR=10

3. Section 3

4. Conclusions

Acknowledgments

References

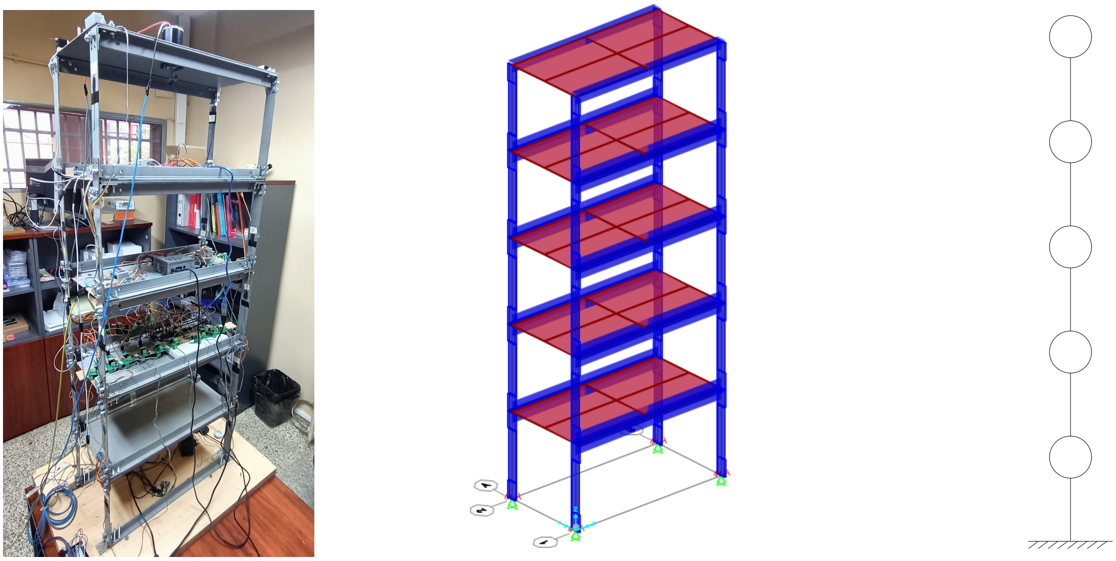

(a) (b) (c)

Figure 1: (a) UGR Frame, (b) HF FE Model, (c) LF Lumped Model.

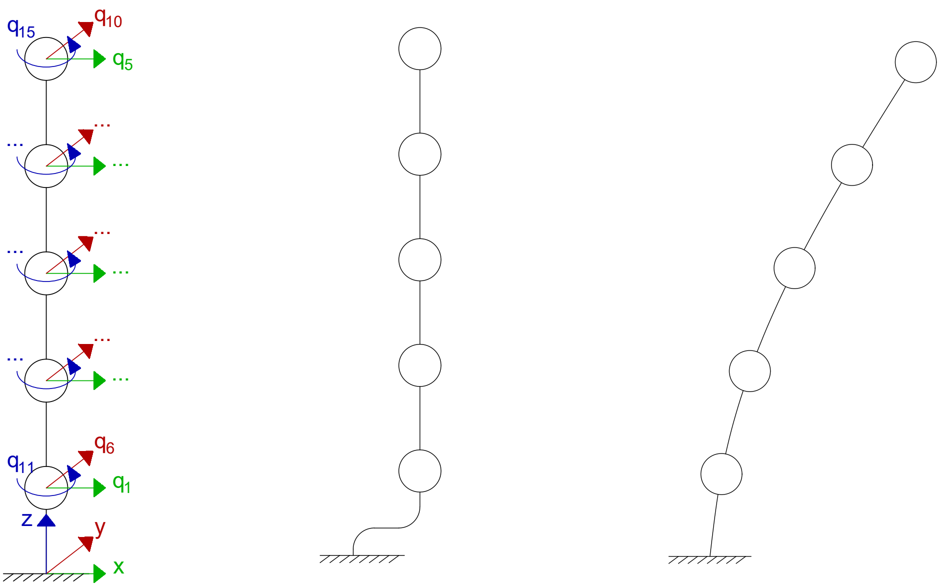

(a) (b) (c)

Figure 2: (a) DOFs of the Lumped Model (b) First mode along X direction (c) First mode along Y direction.

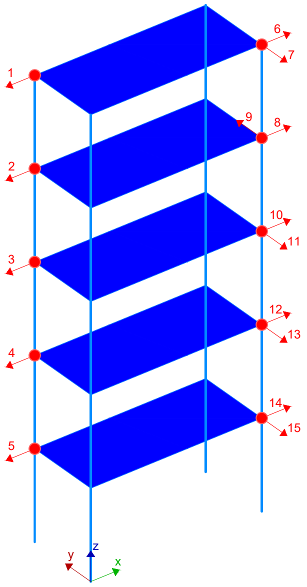

Figure 3: Final DOFs for generated signals